Experimental Study of Reaction in a Partially Wetted Catalytic Pellet

Gregory A. Funk, Michael P. Harold, and Ka M. Ng
Dept. of Chemical Engineering, University of Massachusetts, Amherst, MA 01003

A single-pellet reactor has been used to investigate the impact of partial external wetting on catalyst performance in a multiphase reaction system. The novel design simulates the local environment within a trickle-bed reactor, and permits the direct measurement of the degree of wetting under reaction conditions. Experimental data of the hydrogenation of α-methylstyrene (AMS) over a Pd/Al_2O_3 pellet provide unequivocal evidence of effectiveness enhancement by partial wetting, a predicted single-pellet phenomenon (e.g., Harold and Ng, 1987; Funk et al., 1988, 1989). The overall reaction rate is an increasing (decreasing) function of the degree of wetting if the overall limiting reactant is more effectively supplied through the wetted (nonwetted) part of the surface. A maximum in the reaction rate can occur at an intermediate degree of wetting, signaling a transition from an overall AMS-limited to hydrogen-limited reaction. The dependence of the degree of wetting on the liquid flow rate for low reaction rates is consistent with a simple rivulet flow model. At higher reaction rates the degree of wetting decreases, with all other conditions fixed. Possible mechanisms for this interesting link between the degree of wetting and reaction are discussed.

Introduction

Trickle-bed reactors are used for carrying out a variety of multiphase reactions such as hydrogenations and oxidations. They have been the subject of a large number of studies, many of which are summarized in the reviews of Mills and Dudukovic (1984), Herskowitz and Smith (1983), Van Landeghem (1980), Gianetto et al. (1978), and Satterfield (1975). Despite their widespread use, however, many questions regarding fundamental behavior remain unresolved, due in part to the complex gas-liquid flow.

In the trickling flow regime, the liquid mainly travels down the column on the surfaces of the packings as films or rivulets, while the gas flows through the remaining void space. At sufficiently low liquid flow rates, the external surfaces of the individual catalyst pellets may be covered only partially with liquid. Other more complicated features include liquid filaments, pockets, and pendular structures (Ng and Chu, 1987). Most experimental studies of the trickle-bed reactor were performed using either a differential or lab-scale unit containing many catalyst particles (Sedricks and Kenney, 1973; Satterfield and Ozel, 1973; Germain et al., 1974; Morita and Smith, 1978; Herskowitz et al., 1979; Mata and Smith, 1981; Herskowitz and Moseri, 1983; Tukac et al., 1986; Leung et al., 1987; Ruecker and Akgerman, 1987; Ring and Missen, 1989; among others). Unfortunately, due to the complex flow, these studies provided limited insight into the impact of these important local phenomena on catalyst performance.

The degree of wetting or wetting efficiency, i.e., the fraction of external surface covered by flowing liquid, is an important factor affecting reactor performance (Mears, 1974; Herskowitz et al., 1979; Leung et al., 1987; Ring and Missen, 1989). Consider the common case of reaction between a rather nonvolatile reactant and a sparingly soluble, volatile reactant. The less volatile reactant is supplied primarily to the pellet directly from the liquid film flowing over the pellet surface. Due to its low volatility, its supply rate to the nonwetted surface is relatively low. The volatile reactant traverses two different paths. It can dissolve into and diffuse through the liquid film to the pellet surface, or take a more direct route from the gas to the nonwetted surface. Its supply rate to the nonwetted surface is typically much larger than on the wetted surface.

Previous experimental results suggest that the differences in

Correspondence concerning this article should be addressed to M. P. Harold.
Current address of G. A. Funk: U. O. P. Research Center, Des Plaines, IL 60017.

the external mass transport fluxes can cause an interesting dependence of the overall rate on the liquid flow rate in the partial wetting regime (Satterfield et al., 1969; Herskowitz et al., 1979; Leung et al., 1987). At sufficiently high liquid flow rates, the catalyst pellets are covered completely by liquid. The combination of an incompletely saturated (with volatile reactant) liquid rivulet and a rapid reaction leads to a rate which is limited by the external supply rate of the volatile reactant. As the liquid flow rate is decreased to the point at which there is insufficient liquid to wet the entire catalyst surface, the volatile reactant proceeds to enter the catalyst pores through the nonwetted part. With a subsequent increase in the supply rate of the gaseous reactant, the rate increases. This phenomenon is referred to as *effectiveness enhancement by partial wetting* (Harold and Ng, 1987). If the flow rate is lowered below some critical level, the fraction of surface wetted by the liquid is sufficiently low that the nonvolatile reactant becomes limiting. Without an adequate supply of nonvolatile reactant, the rate continues to decline with further decreases in the degree of wetting.

This description assumes that the flowing liquid is a well defined rivulet and that each particle is exposed to such a rivulet. Due to the random nature of the bed and an imperfect liquid-inlet distribution, however, each particle in the bed may be exposed to a different local environment: degree of wetting, number and position of liquid films, type of flow feature, etc. As a result, the true impact of the partial wetting phenomenon is masked at least partially by the complex flow pattern. Therefore, experimental reactor designs that clarify the local picture are essential.

Many investigators have resorted to mathematical models of the single, partially-wetted catalyst to study various interacting processes. Until recently, these diffusion-reaction models were based on the assumption that a single reactant limits the reaction under all wetting conditions throughout the entire pellet: the pseudofirst-order kinetics approximation (Dudukovic, 1977; Ramachandran and Smith, 1979; Herskowitz et al., 1979; Herskowitz, 1981; Goto et al., 1981; Sakornwimon and Sylvester, 1982; Capra et al., 1982). For reasons discussed earlier, these models are incapable of predicting an overall reaction rate maximum at an intermediate liquid flow rate. This led to the development of models with more realistic bimolecular rate expressions such as a first-order dependence on both the gas reactant and the liquid reactant (Gabitto et al., 1986; Yentekakis and Vayenas, 1987; Funk et al., 1988). Funk et al. showed that under certain conditions there may be regions within the catalyst with different limiting reactants and that both interparticle and intraparticle mass transport can be rate-limiting in these regions. Funk et al. (1989) considered models with more realistic kinetic rate expressions.

There is a definite need to experimentally confirm these single-pellet model predictions and to better understand trends observed in previous lab-scale reactor experiments. Given this need, we opted for a single-pellet reactor design, in which the liquid flow is well defined. In this study, a novel single-pellet reactor is employed, in which the wetting efficiency of a single or two flowing rivulets is controllable and directly measurable under reaction conditions. Rivulet flow with incomplete wetting is investigated since it is the least complex of the flow features mentioned above. Certainly, multipellet features such as liquid pockets deserve attention in future studies. The hydrogenation of α-methylstyrene to cumene over a supported Pd catalyst was chosen as the test reaction since it is representative of a large class of commercially important multiphase reactions.

Experimental Setup and Procedures

The multiphase reaction was carried out in a glass vessel containing a single, cylindrical catalytic pellet that was suspended vertically from a wire, as shown in Figure 1. A liquid-phase reactant was injected onto the side of the pellet from a stainless steel tube and flowed down the external surface of the pellet as a thin rivulet. The 0.18-cm-ID inlet tube was positioned at a vertical angle of approximately 15° such that the tip of the tube slightly contacted the pellet 0.5 cm from the top. Gas entered at the bottom of the reactor and flowed countercurrently. It should be pointed out that although this is the opposite direction than that for the gas phase in a cocurrent downflow trickle bed, we do not expect the results to be different because of the short contact time of the gas.

Compared to other multiphase reactions, the hydrogenation of α-methylstyrene (AMS) to cumene over a Pd/Al_2O_3 catalyst is rather fast under mild operating conditions. This reaction system has been utilized in a number of previous trickle-bed reactor studies (e.g., Satterfield et al., 1969; Germain et al., 1974; Morita and Smith, 1978; Herskowitz et al., 1979; Turek and Lange, 1981). All of the results presented below were obtained at 40°C and 1 atm. Under these conditions, AMS is rather nonvolatile, hydrogen is only slightly soluble in AMS, the reaction is irreversible, and side reactions are not important.

The glass reaction vessel was surrounded by an annular water jacket to prevent condensation on the walls of the vessel. This also provided for a more isothermal environment. The pellet

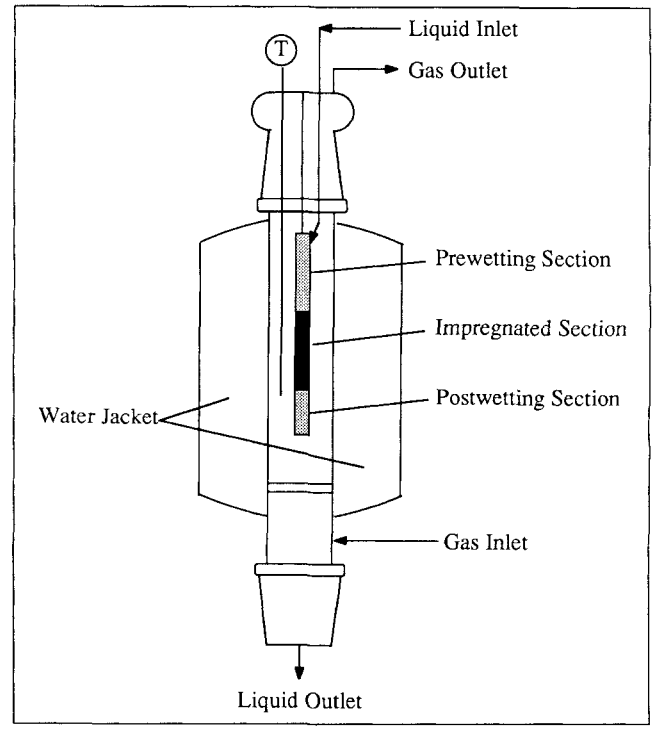

Figure 1. Single-pellet reactor.

was positioned inside the reactor so that the middle active section was in the center of the water jacketed portion. The reactor temperature was monitored by a thermocouple positioned approximately 0.2 cm from the external pellet surface and was controlled using a heating cord wrapped around the outside of the water jacket. (For clarity, the heating cord is not shown in the schematic.)

Since the entire vessel was constructed of glass, it was possible to directly measure the fractional liquid coverage under reaction conditions. By positioning a fluorescent light above the pellet and viewing from below, the surface of the liquid film appeared glossy, whereas the nonwetted region was dull. The contact line between the two regions was clearly visible to the naked eye. Sixteen equally-spaced markings around the circumference of the pellet, both above and below the active section, provided a scale to estimate the rivulet width. In addition to the single-tube inlet, a double-tube inlet configuration was also used. In this case, the liquid was split into two equal streams using two precision needle valves and injected on diametrically opposite sides of the pellet.

The porous catalyst pellet had a uniform diameter of 0.8 cm and comprised three different sections that were glued together using an epoxy cement (Devcon, 5 Minute Epoxy Gel). The same adhesive was used to attach the pellet to the stainless steel wire suspending the pellet. The top section was made of an inactive γ-alumina-clay mixture (described below). It served as an entrance length region for the injected liquid flow to develop before passing over an active middle section, which consisted of the same alumina-clay mixture impregnated with 1.25 wt. % Pd. Both of these sections were 6 cm in length. Another 2.5 cm section of unimpregnated alumina-clay was attached at the bottom of the middle section to minimize the effects of liquid dripping off the pellet.

The alumina-clay supports used in all three sections were made by compressing a dough, consisting of pseudoboehmite alumina, attapulgite clay, and distilled water in a cylindrical die. After drying, the samples were calcined at 625°C for 1 hour. Standard techniques were used to impregnate the middle section with Pd. Complete details and a more thorough discussion of the support fabrication are provided elsewhere (Funk, 1990). The physical properties of the catalyst are listed in Table 1. Visual inspection indicated that the Pd was distributed fairly uniformly. This observation was confirmed with a scanning electron microprobe analysis performed by the Mobil Research and Development Company. Typical results are provided by Funk (1990).

Figure 2 shows the overall experimental setup. A gas phase consisting of pure hydrogen or pure nitrogen was delivered to the reactor at a constant rate of 1.67 cm^3/s using mass flow controllers. Both the nitrogen and hydrogen (Aero All Gas) had purities of at least 99.99% and 99.9%, respectively. The gas was preheated with heating cords wrapped around the stainless steel line.

Table 1. Physical Properties of Catalyst Used in Study

Surface area = 1.18×10^5 m^2/kg
Pellet density = 840 kg/m^3
Solid density = 1,990 kg/m^3
Void fraction = 0.583
Average pore chamber radius = 2.12×10^{-8} m
Average pore mouth radius = 7.99×10^{-9} m

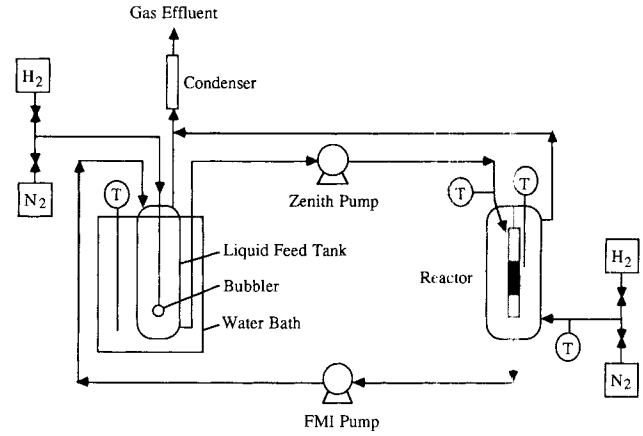

Figure 2. Experimental setup.

All of the experiments were performed using total recycle of the liquid phase, which consisted of α-methylstyrene (AMS) or a mixture of AMS and mesitylene (1, 3, 5 trimethylbenzene). Both liquids were acquired from Kodak and had purities of at least 98%. Before an experiment, the AMS was soaked in a flask containing 10 g of γ-Al_2O_3 pellets to remove the polymerization inhibitor, p-tert-butylcatechol. A Zenith (model BPB) gear pump was used to deliver a smooth, pulseless liquid flow to the reactor from a 150 mL feed tank. The insulated stainless steel tubing connecting the feed tank and the reactor was heated to insure that the liquid entering the reactor was at the same temperature as the bulk gas temperature. After flowing over the pellet, the liquid was recycled back to the feed tank. To keep the contents of the feed tank at a constant temperature of 40°C, this entire unit was submersed in a water bath. In some experiments, hydrogen was bubbled through the tank to presaturate the liquid. Nitrogen was used in other experiments to strip hydrogen from the liquid. For these latter cases, the liquid feed is referred to as "unsaturated." Although the dissolved hydrogen concentration was not measured, the two extremes of bubbling hydrogen or nitrogen in the stirred liquid came close to providing a fully saturated (with hydrogen) liquid feed and one which was nearly devoid of hydrogen. A condenser installed at the gas outlet recovered any liquid which vaporized. Water served as the cooling fluid.

The overall reaction rate was determined by measuring the buildup of cumene in the liquid phase. Small samples of the liquid were withdrawn from the feed tank and analyzed using gas chromatography after sufficient time passed (4–6 hours) for the pseudosteady concentration profiles to be established. The gas chromatograph (Hewlett-Packard model 5890) was operated in the splitless mode with a capillary column (J&W, Durobond Wax) and flame ionization detector. Peak areas were calibrated using the method of internal standardization. The concentration of cumene was monitored as a function of time. If the single-pass conversion and total conversion for the run are low, a straight line should result. The overall, or observed, rate was calculated using the batch-recycle equation (Morita and Smith, 1978):

$$r_{obs} = \frac{V_{liq}}{m_{cat}} \left(\frac{dC}{dt}\right)_{cumene} \tag{1}$$

where V_{liq} is the average volume of liquid in the system over

the sampling period, m_{cat} is the mass of active catalyst, C is cumene concentration, and t is time. An observed linear dependence of C on time (i.e., constant slope) implied that a pseudosteady state had been achieved. The statistical uncertainty in the slope of the cumene concentration vs. time data, which was evaluated using linear least squares, was estimated using standard methods (Shoemaker et al., 1981). For all of the results presented below, the percent uncertainty in the reported value of the reaction rate was always less the $\pm 12\%$ based on a confidence limit of 95%. In general, the magnitude of the percent uncertainty decreased with increases in the reaction rate. In one of the plots shown below, error bars are provided for several of the data points to illustrate the degree of uncertainty in that data set.

Experimental Results

Single-pellet reactor experiments were conducted over a range of different operating conditions. All of the experiments were carried out at 40°C and 1 atm. The variables considered were:

- Liquid inlet configuration (single or double inlet)
- Liquid flow rate
- Gas-phase composition (hydrogen or nitrogen)
- Degree of hydrogen saturation of liquid entering the reactor
- Liquid composition (AMS in mesitylene).

For a specific set of conditions, the overall rate of α-methylstyrene hydrogenation and the wetting efficiency were measured as a function of volumetric liquid flow rate.

The same catalyst pellet was used in all the experiments. This permitted direct comparisons among different experiments. The consistency of the data indicates that the experiment was quite reproducible and that catalyst deactivation was insignificant.

This section is divided into two parts: 1. the data obtained with the double-tube inlet and 2. the single-tube inlet results. The single-tube inlet offers the advantage of a single liquid film. Due to hydrodynamic factors considered in the Analysis and Discussion section, however, the maximum wetting efficiency attainable with this inlet was only about 50%. The double-tube inlet design enabled the degree of wetting to be varied from about 20% to 100%.

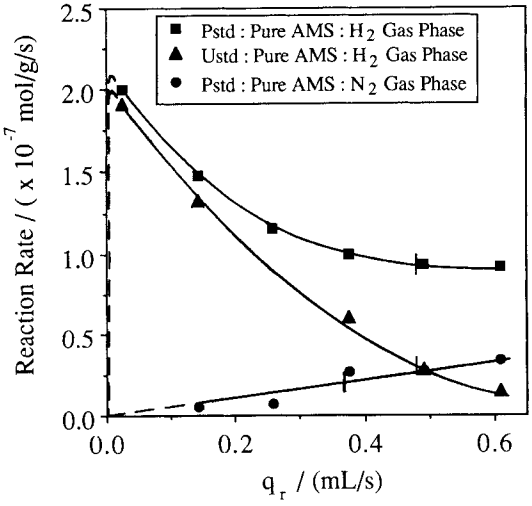

Figure 3. Effect of liquid flow rate on reaction rate for the double-tube inlet.

Hash marks on curves indicate critical flow rate for complete wetting.

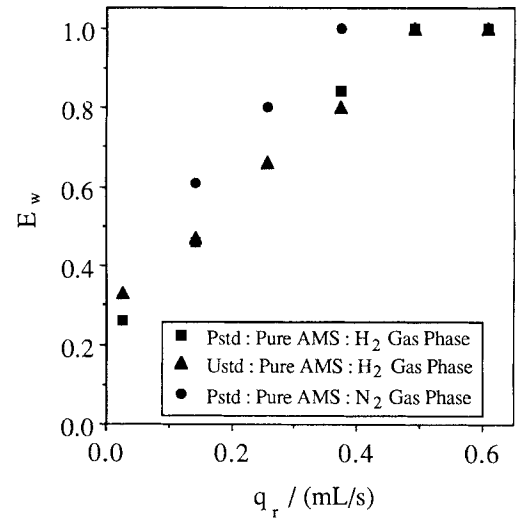

Figure 4. Effect of liquid flow rate on wetting efficiency for the double-tube inlet.

Double-tube inlet

In the first set of experiments, the impact of the hydrogen supply rate on the catalyst performance was investigated. Figures 3 and 4 show the dependence of the reaction rate and wetting efficiency on liquid flow rate, respectively, and Figure 5 the reaction rate dependence on wetting efficiency, for different combinations of gas- and liquid-phase compositions. In all the experiments, the liquid phase was pure α-methylstyrene. The squares in each figure represent the results obtained with a presaturated liquid feed and a pure hydrogen gas phase. The experiments represented by triangles were performed under identical conditions except that the liquid feed was not presaturated with hydrogen, i.e., the inlet liquid had a lower

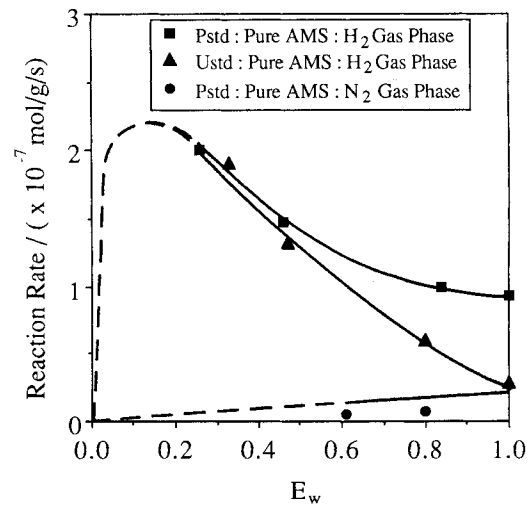

Figure 5. Dependence of reaction rate on wetting efficiency.

All experiments were performed with the double-tube inlet.

concentration of hydrogen. Finally, the circles show the results for a presaturated liquid feed but a nitrogen gas phase. Under these conditions, hydrogen entered the reactor only with the incoming liquid. Note that the filled symbols indicate the double-tube inlet runs. Data obtained with the single-tube inlet are represented with unfilled symbols below. Solid lines drawn through the points indicate an approximate fit; dashed lines show our own interpreted extrapolation of the trends where there are insufficient data. All of the rate curves are extrapolated to a zero rate when there is no liquid flowing since this corresponds to a case in which no AMS is supplied to the reactor.

Figure 3 shows that for the case of a nitrogen gas phase (circles), the reaction rate increases monotonically with increasing liquid flow rate. In contrast, both of the hydrogen gas-phase experiments (squares and triangles) exhibit a distinct maximum in the reaction rate. With the exception of the highest flow rate, the reaction rate was highest for the hydrogen saturated liquid case, followed by the unsaturated liquid and nitrogen cases. It was not possible to pinpoint the magnitude or location of this maximum, since it occurred at a flow rate below the minimum flow rate that we could achieve. The hash mark placed on each curve denotes the approximate flow rate at which complete wetting was observed.

Figure 4 shows how the wetting efficiency varied with liquid flow rate for these experiments. As expected, increases in the liquid flow rate resulted in increases in the liquid coverage. However, a key point is that the coverage sharply increases at the lowest flow rates ($q_r < 0.1$ mL/s), then more gradually increases up to complete wetting. For a given flow rate, the wetting efficiency of the nitrogen gas-phase experiments was consistently higher in the partial wetting regime. We will return to this point in the Analysis and Discussion section. The data contained in Figures 3 and 4 are replotted in Figure 5 to show the relation between the two dependent variables—reaction rate and wetting efficiency.

A second set of experiments demonstrate the impact of the

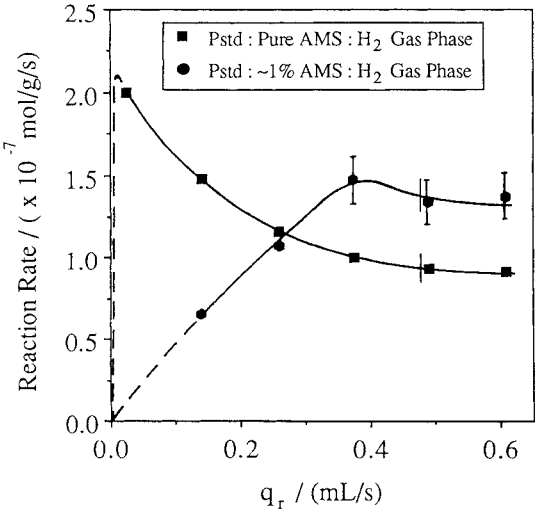

Figure 6. Comparison of reaction rate dependence on liquid flow rate for pure AMS and 1% AMS liquid feeds.

Both experiments were performed with the double-tube inlet. Hash marks on curves indicate critical flow rate for complete wetting.

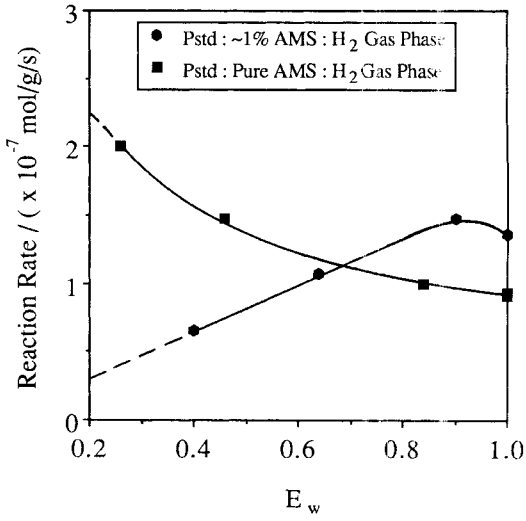

Figure 7. Comparison of reaction rate dependence on wetting efficiency for pure AMS and 1% AMS liquid feeds.

Both experiments were performed with the double-tube inlet.

AMS supply on the catalyst performance (Figures 6-8). In Figures 6 and 7, the hexagons show the dependence of the rate on the liquid flow rate and wetting efficiency, respectively, for the case of a hydrogen presaturated liquid feed comprised of approximately 1 wt. % AMS in mesitylene. The gas phase was pure hydrogen. The corresponding pure AMS results (squares) are replotted for comparison. At high liquid flow rates (Figure 6) or liquid coverages (Figure 7) the diluted AMS experiments give a higher rate of reaction. In addition, as the concentration of AMS is decreased, the maximum reaction rate shifts to a higher liquid flow rate or wetting efficiency. In Figure 6 we have drawn the solid line for the diluted AMS rate data as a slightly decreasing function of liquid flow rate for $q_r > 0.4$ mL/s. However, we have included error bars on these three data points to indicate that the rate may simply level off in this region.

Figure 8 shows the dependence of the rate on wetting efficiency for the case of a hydrogen unsaturated liquid feed consisting of 4 wt. % AMS in mesitylene with a hydrogen gas phase (inverted triangles). The corresponding pure AMS experiments (from Figure 5) are included for comparison (upright triangles). Similar to the 1 wt. % AMS experiments (Figures 6 and 7), the decrease in the AMS concentration to 4 wt. % results in the rate maximum moving to a higher wetting efficiency. Moreover, the rate is higher with the diluted liquid feed at sufficiently high liquid coverages ($E_w > 0.48$). Again, we will return to these observations in the Analysis and Discussion section.

Single-tube inlet

The results obtained with the single-tube inlet are contained in Figures 9-11. Figures 9 and 10 show the dependence of the reaction rate and the wetting efficiency on the liquid flow rate, respectively. These data are replotted in Figure 11 to show the relation between the rate and wetting efficiency. In all three of these figures, squares are used to represent the experiments with a presaturated, pure AMS liquid phase and a pure hy-

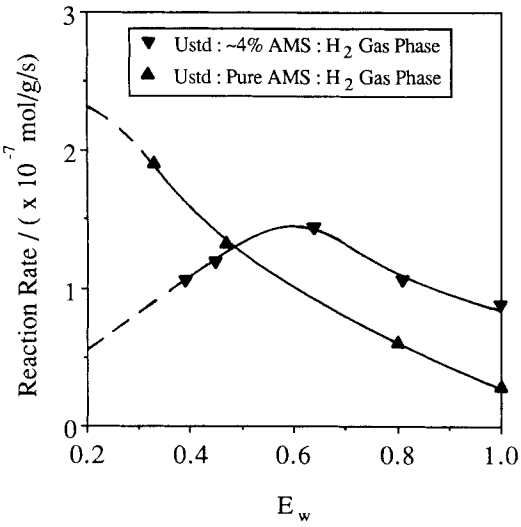

Figure 8. Comparison of reaction rate dependence on wetting efficiency for pure AMS and 4% AMS liquid feeds.

Both experiments were performed with the double-tube inlet.

drogen gas phase. The results represented by triangles were obtained under the same conditions except that the liquid feed was not saturated with hydrogen. Circles show the behavior observed for a presaturated, pure AMS liquid phase, but a pure nitrogen gas phase. Finally, the experiments represented with diamonds show the impact of changes in the liquid-phase composition. In these runs, the liquid phase was a hydrogen unsaturated mixture of approximately 1 wt. % AMS in mesitylene, and the gas phase was pure hydrogen.

As in the double-inlet experiments at low liquid coverages, the rates are highest when the gas phase is pure hydrogen and liquid phase is pure AMS (squares and triangles in Figures 9 and 11). If the liquid feed is presaturated with hydrogen (squares), the reaction rate is essentially independent of the liquid flow rate (or wetting efficiency). For the case of an unsaturated liquid feed, however, the reaction rate exhibits a

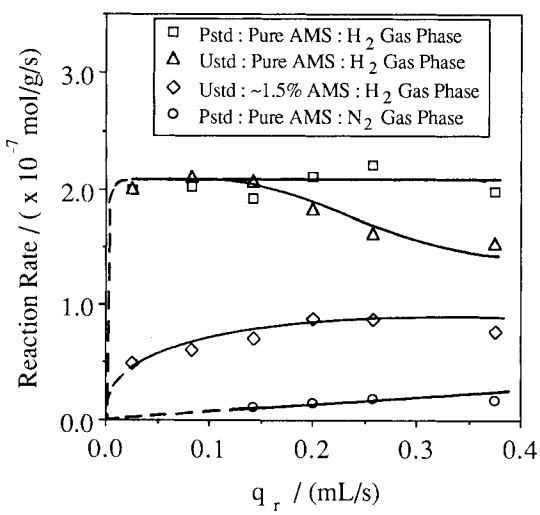

Figure 9. Effect of liquid flow rate on reaction rate for the single-tube inlet.

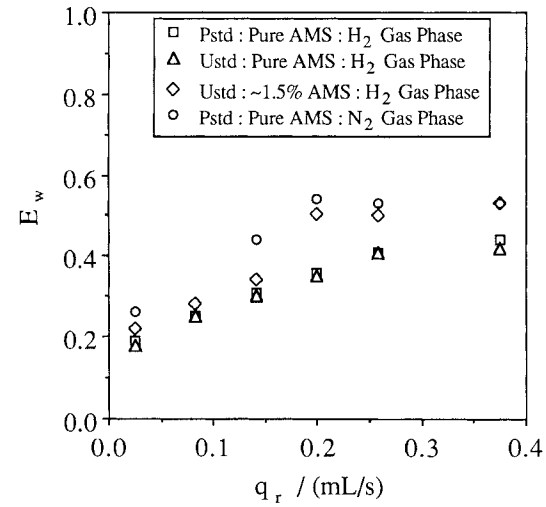

Figure 10. Effect of liquid flow rate on wetting efficiency for the single-tube inlet.

slight decline at the highest liquid flow rates considered. If the gas phase is nitrogen, the rate is much lower and increases with increasing liquid flow rate. In general, the rate obtained with the 1 wt. % AMS also increases with increasing liquid flow rate (or wetting efficiency). At the highest liquid flow rates, the reaction rate levels off. This trend, which is also true for the double inlet experiments, is due to rather weak dependence of the wetting efficiency on liquid flow rate in this region. Figure 10 shows that the wetting efficiency increases rapidly at low flow rates, but plateaus at the highest liquid flow rates considered in these experiments. This causes the rate to be rather insensitive to changes in the flow rate at high q_r.

Analysis and Discussion

Before considering the catalyst performance under partially wetted conditions, it is instructive to estimate the extent of transport limitation for the case of a fully wetted pellet. With-

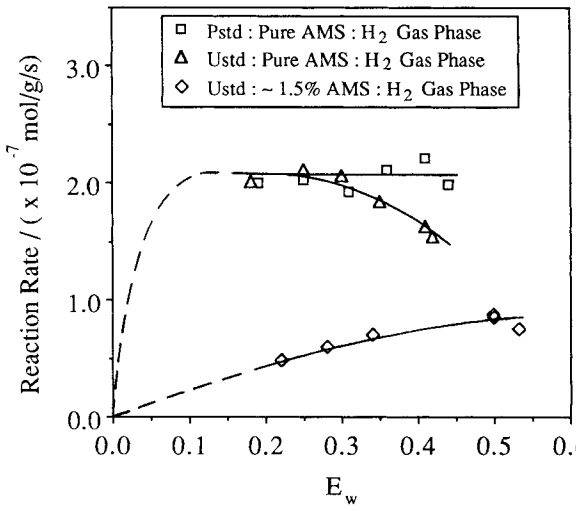

Figure 11. Dependence of reaction rate on wetting efficiency.

All experiments were performed with the single-tube inlet.

out detailed knowledge of the intrinsic kinetics, the observable Weisz-Prater modulus Φ (Weisz and Prater, 1954) is used to estimate the diffusional intrusion; Φ is given by

$$\Phi = \left(\frac{R_p}{2}\right)^2 \frac{r_{obs}\rho_p}{D_{eH}C_{bH}} \tag{2}$$

where R_p and ρ_p are the pellet radius and apparent density, r_{obs} is the observed rate (per unit mass of catalyst), and D_{eH} and C_{bH} are the dissolved hydrogen effective diffusivity and bulk liquid film concentration, respectively. If $\Phi > 1$, then diffusional limitations are important. Using an observed reaction rate of 10^{-7} mol/(g cat·s) under complete wetting conditions, Figure 5, $R_p = 0.4$ cm, $D_{eH} \approx 10^{-5}$cm^2/s (an estimate), $C_{bH} = 3 \times 10^{-6}$ mol/cm^3 (measured solubility of hydrogen in pure AMS; see discussion later), and $\rho_p = 0.84$ g/cm^3 (measured; see Table 1), gives $\Phi = 110$. This indicates that diffusional limitations of the limiting reactant hydrogen are severe. As we discuss below, transport limitations of the AMS may also become important under some conditions.

Hydrogen supply limitations

Over nearly the entire range of wetting efficiency, the supply of hydrogen to the partially wetted pellet is clearly the most critical process if the AMS is in large excess, as is the case in the pure AMS experiments (e.g., Figures 3 and 5). Note that the solubility of hydrogen in pure AMS at 40°C is approximately 3×10^{-6} mol/cm^3, which is considerably less than the AMS molar concentration of approximately 7.5×10^{-3} mol/cm^3. For the double-tube inlet system, Figure 3 shows that the highest reaction rates are obtained at the lowest nonzero liquid flow rates achieved in the experiments with a pure hydrogen gas feed. This also corresponds to the lowest measurable wetting efficiencies (Figure 4). As the flow rate is increased from this point, the rate declines monotonically for the two hydrogen gas experiments. These data clearly demonstrate the effectiveness enhancement by partial wetting phenomenon (Harold and Ng, 1987; Funk et al., 1988, 1989). In effect, by covering more of the surface with the flowing liquid, the supply rate of the limiting reactant hydrogen is reduced, since the supply of hydrogen into the liquid-filled pores is deterred by the flowing liquid film. This effect is quite dramatic if the feed liquid is not presaturated with hydrogen. Indeed, Figure 5 shows that the rate under fully wetted conditions is approximately one-tenth the maximum rate obtained when the pellet is only 25% wetted.

If nitrogen replaces hydrogen in the gas, the rate is a weak, increasing function of the flow rate (or degree of wetting) since the sole hydrogen supply route to the pellet is from the inlet liquid (Figures 3, 5, and 9). In this case, the partially wetted pellet performs worse than the fully wetted pellet.

Some of the more subtle features of the data in Figures 3-5 also deserve discussion. The rates obtained for the presaturated (squares) and unsaturated liquid (triangles), pure hydrogen gas-phase experiments converge as the liquid flow rate is decreased (see Figures 3 and 5 for the double inlet experiments and Figures 9 and 11 for the single inlet experiments). At the lowest flow rate, the reaction rates for the two cases are nearly identical. Most likely reason for this behavior is that most of the hydrogen which reacts enters through the nonwetted surface. As a result, the liquid composition has only a negligible impact on the rate.

Under fully wetted conditions (i.e., to the right of the hash marks in Figure 3), the overall rate may be either an increasing or decreasing function of liquid flow rate, depending on the reactor conditions. The hydrogen supply rate depends on the film thickness and the extent to which its profile is established along the length of the pellet. For example, the rate increases with increasing liquid flow rate for the hydrogen-saturated liquid, pure nitrogen gas-phase case (circles). Since hydrogen is supplied only to the reactor with the liquid, increases in the liquid flow rate provide a greater supply of the limiting hydrogen along the entire pellet length. Moreover, the liquid-to-solid mass transfer coefficient is an increasing function of q_r (Funk et al., 1990). Another possible contributing factor is a reduction in the desorption of hydrogen into the nitrogen gas phase because of the shorter contact time between the liquid film and gas. All of these factors lead to a higher reaction rate. In contrast, in the unsaturated liquid, pure hydrogen gas-phase experiments (triangles), the rate decreases with increasing q_r under complete wetting conditions. In this case, the supply rate of hydrogen from the gas phase is critical, due to the very low hydrogen concentration in the feed liquid. As the liquid flow rate is increased, the liquid velocity and film thickness increase, while the contact time between the liquid and the gas phase decreases. As a result, the amount of limiting hydrogen that can diffuse through the film to the pellet decreases, and consequently, so does the rate. On the other hand, for the hydrogen-presaturated liquid, hydrogen gas-phase case (squares), an increase in the liquid flow rate supplies the limiting hydrogen more effectively along the entire length of the pellet, but also deters the supply of hydrogen from the gas. These opposing effects apparently balance so that the overall rate is essentially independent of the degree of wetting.

AMS supply limitations

In the hydrogen gas-phase experiments, the supply of the liquid-phase reactant (AMS) limits the overall rate if either the degree of wetting or the bulk AMS concentration is reduced sufficiently. The key reason is that AMS is relatively nonvolatile. With a vapor pressure of 600 N/m^2 at 40°C, an upper bound on the gas-phase mole fraction of AMS is only 0.59% (since the gas flows continuously). The rate maximum at an intermediate flow rate can be interpreted as a transition from a hydrogen to AMS-limited state. Unfortunately, in the pure AMS experiments, an actual rate maximum was not measured (Figures 3-5), since flow rates below 0.025 mL/s could not be obtained accurately. Nevertheless, since the trivial zero liquid flow experiment gives a zero steady-state rate, this infers the existence of a rate maximum. The maximum rate occurs at such low wetting efficiencies in the pure AMS experiments because of the large excess of AMS in the liquid phase. These features confirm the model predictions of Harold and Ng (1987) and Funk et al. (1988, 1989).

If the liquid-phase AMS concentration is reduced significantly by dilution in mesitylene, the range over which the rate is limited by the supply of AMS is enlarged. This is demonstrated in Figures 6 and 9 in which the rate is an increasing function of the liquid flow rate (degree of wetting) (Figures 7, 8, and 11). Compare this trend to the results obtained in ex-

periments under identical conditions but with a pure AMS feed. In the latter case, the rate is significantly higher and has a negative slope in the same flow rate range. The diluted AMS data infer that a higher coverage of the liquid supplies more AMS to the AMS-starved pellet. Again, the maximum in the rate clearly reveals the transition from an AMS-limited to a hydrogen-limited state. The degree of wetting giving the maximum moves to higher values as the AMS to hydrogen concentration ratio is reduced. The results also confirm previous model predictions (Harold and Ng, 1987; Funk et al., 1988).

Another interesting result was obtained in the diluted AMS experiments: the overall rate obtained under fully wetted conditions with diluted AMS is higher than the fully wetted rate obtained with pure AMS. For example, in the presaturated runs (Figure 7) the rate is about 40% higher for the 1% AMS feed compared to a pure AMS feed. In the absence of mass transport effects or changes in hydrogen solubility with liquid composition and for the case of bimolecular first-order kinetics, the rate should vary proportionally with the AMS concentration. However, as we now demonstrate, nonlinear kinetics, transport effects, and solubility each contribute to an apparent negative order with respect to AMS.

In our laboratory AMS hydrogenation was recently carried out under conditions of minimal mass transport limitations (Cini et al., 1989). The catalyst consisted of Pd deposited in a supported γ-Al_2O_3 film of approximately 50 μm thickness. The Pd loading in the film was approximately 2 wt. %. At 40°C and 1 atm, the rate dependence on AMS concentration (in mesitylene) exhibited a shift from positive order to zero order as the AMS concentration was varied from 1 wt. % to 100 wt. %. The rate was nearly zeroth-order for AMS concentrations exceeding 8 wt. %. The zeroth-order rate dependence has been observed in previous studies involving AMS hydrogenation over supported Pd catalysts (e.g., Satterfield et al., 1969; Herskowitz et al., 1979; Turek and Lange, 1981). The functional form is correlated well by the rate expression:

$$r_{\text{int}} = \frac{k_r K_A C_A C_H}{1 + K_A C_A} \tag{3}$$

where k_r is a surface rate constant, K_A is the absorption equilibrium constant, and C_A and C_H are the concentrations of AMS and hydrogen, respectively. A similar expression was proposed by Turek and Lange (1981).

An analysis using this rate expression is now carried out to help explain the data. The observed rate of reaction between hydrogen and AMS in a fully wetted catalytic pellet of volume V_p and external surface area S_x is given by

$$r_{\text{obs}} = \eta r_{\text{int}}(C_{bA}, C_{bH}) \tag{4}$$

where $r_{\text{int}}(C_{bA}, C_{bH})$ is the intrinsic rate evaluated at the bulk conditions (C_{bH} is the equilibrium solubility of hydrogen and C_{bA} the bulk AMS concentration), and η is the overall effectiveness. If AMS is in large excess, the rate is first-order in hydrogen and zeroth-order in AMS (Eq. 3). We note that $C_{bA} >> C_{bH}$ is satisfied even for a 1 wt. % AMS mixture (i.e., $C_{bA}/C_{bH} \approx 25$). Thus, η can be approximated by the formula for a unimolecular first-order reaction (Froment and Bischoff, 1979):

$$\frac{1}{\eta} = \frac{\phi}{\tanh\phi} + \frac{\phi^2}{Sh'} \tag{5}$$

where ϕ is the Thiele modulus defined by

$$\phi = \left(\frac{V_p}{S_x}\right)\sqrt{\frac{k'}{D_{eH}}} \tag{6}$$

and k' is a pseudofirst-order rate constant defined as

$$k' = \frac{k_r K_A C_{bA}}{1 + K_A C_{bA}} \tag{7}$$

Sh' is the modified Sherwood number defined by

$$Sh' = \left(\frac{V_p}{S_x}\right)\frac{\epsilon k_{gls}}{D_{eH}} \tag{8}$$

where ϵ is the particle porosity and k_{gls} is an overall mass transport coefficient (for hydrogen). Note that Sh' lumps three external transport steps: bulk gas-to-gas/liquid interface, gas/liquid interface-to-bulk liquid, and bulk liquid-to-solid surface. Thus, η is an overall effectiveness that is dependent on the bulk flows. Any detailed model of this system certainly would require the separation of these transport steps in a heterogeneous formulation. For example, the reader is referred to Harold et al. (1989) who simulated the string-of-pellets data of Satterfield et al. (1969).

Table 2 provides the overall rate expression (r_{obs}) for three limiting cases: (i) reaction control, (ii) intraparticle diffusion control, and (iii) external transport control. Again, in case (i) the apparent order shifts from unity at low C_{bA} to zero at high C_{bA}. In case (ii) the apparent order changes from 0.5 at low C_{bA} to zero at high C_{bA}. In case (iii) the apparent order is zero for all C_{bA}. Thus, at high AMS concentrations the zero-order AMS dependence is unchanged by mass transport. For a sufficiently low bulk concentration of AMS (below 5 wt. %), the apparent reaction order depends on the severity and type of mass transport resistance. Based on an earlier estimate of the Weisz-Prater modulus ($\Phi = 110$) for a fully wetted pellet and a pure AMS feed, we know that the rate is severely limited by mass transport. However, even if the external supply of hydrogen is limiting, the predicted zero-order dependence of the

Table 2. Overall Rate Expressions and Apparent Orders with respect to AMS for Three Limiting Cases*

Case	Observed Rate (r_{obs})	Apparent Order W/R AMS
Reaction control	$\left(\frac{k_r K_A C_{bA}}{1 + K_A C_{bA}}\right) C_{bH}$	0–1
Intraparticle diffusion control	$\left[\sqrt{D_{eH}}\left(\frac{S_x}{V_p}\right)\right]\sqrt{\frac{k_r K_A C_{bA}}{1 + K_A C_{bA}}}\, C_{bH}$	0–0.5
External transport control	$\left[\epsilon k_{gls}\left(\frac{S_x}{V_p}\right)\right] C_{bH}$	0

*The observed rate expression is given by Eq. 4.

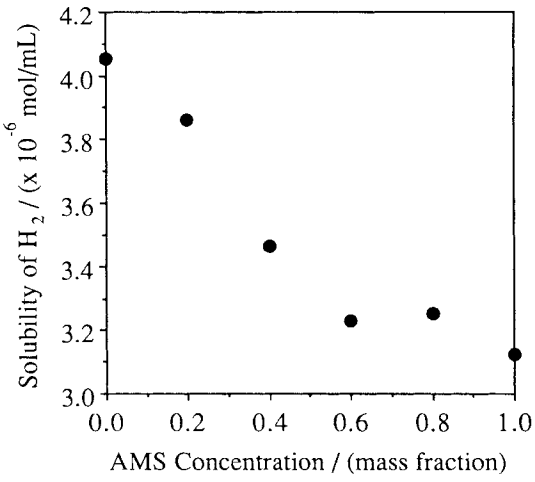

Figure 12. Dependence of hydrogen solubility on the mass fraction of α-methylstyrene with mesitylene as the solvent.

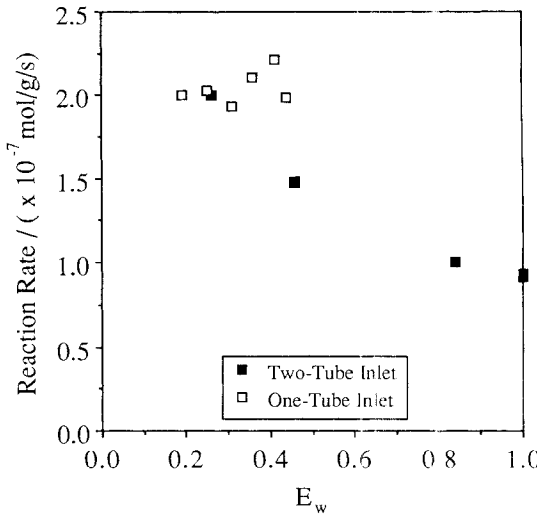

Figure 13. Comparison of reaction rate dependence on wetting efficiency obtained with the single- and double-tube inlets for hydrogen-presaturated liquid feeds.

rate on AMS still cannot explain the observed increase in the overall rate with decreases in the AMS concentration.

The final piece of information concerns the hydrogen solubility. Throughout this analysis it has been implicitly assumed that the solubility is independent of the liquid-phase composition. To investigate this potential factor, the hydrogen solubility was measured for solutions containing AMS and mesitylene with different compositions. Details of the procedure are described by Funk (1990). The final results, which are presented in Figure 12, show the dependence of the hydrogen solubility on the mass fraction of AMS. The hydrogen solubility is a decreasing function of the AMS concentration. In pure mesitylene, H_2 has a solubility approximately 30% greater than in pure AMS.

Pieced together, these findings help explain the apparent increase in the overall rate as the AMS concentration is decreased for the fully wetted pellet. The rate increase is due to the combined effects of increased hydrogen solubility in mesitylene, a negligible intrinsic rate dependence on AMS above 8 wt. % AMS, and operation in a mass transport limited regime. On the other hand, the pronounced positive-order dependence on the AMS in the partially wetted regime demonstrates that the pellet is starved of AMS in regions of the pellet sufficiently removed from the wetted surface.

Number of liquid rivulets

In the trickle-bed reactor a catalytic pellet is likely exposed to more than one film or rivulet. As a first step, it is of interest to determine the impact of the number of flowing films on catalyst performance. One intriguing question is whether the number of films affect the overall rate for a fixed degree of wetting. This and other questions can be addressed by properly comparing the data from the single and double inlet experiments.

Figures 13 and 14 show the dependence of the overall rate on the degree of wetting obtained with the single and double inlet configurations for the experiments in which the pure AMS feed was presaturated and unsaturated with hydrogen, respectively. The E_w range for comparison is limited between 0.2 and 0.45 because of the narrow range covered with the single inlet design. It should be noted that for a fixed degree of wetting the total liquid flow rate required is less for the double inlet than for the single inlet (compare Figures 4 and 10). The reason is rooted in the film flow dynamics discussed below. This flow rate difference is a key factor in explaining the overall trends in the data.

For the presaturated liquid feed (Figure 13), the overall rate is approximately the same for both the single and double inlets at the lowest measured wetting efficiencies ($E_w \approx 0.2$–0.25). At such low flow rates the wetting configuration is not crucial since the primary hydrogen supply route is through the nonwetted surface. As E_w is increased to 0.45, however, the single inlet rate remains constant (within experimental error) but the

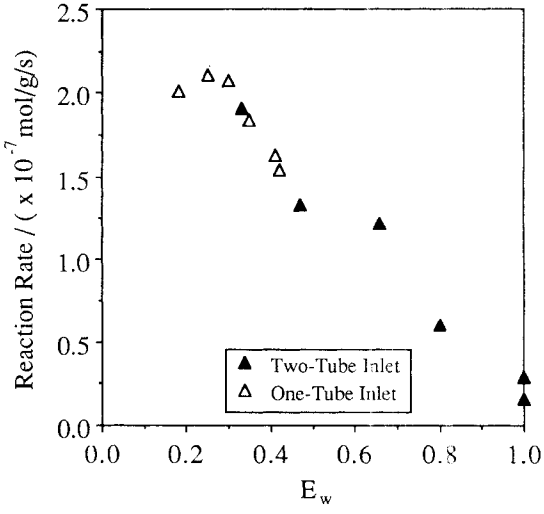

Figure 14. Comparison of reaction rate dependence on wetting efficiency obtained with the single- and double-tube inlets for hydrogen-unsaturated liquid feeds.

double inlet rate decreases sharply. The cause of this behavior is attributed to the fact that a single inlet flow rate of approximately 0.26 mL/s is needed to give $E_w = 0.4$ compared to 0.1 mL/s for the double inlet (Figures 4 and 10). For the single-tube inlet, the higher liquid flow rate more effectively provides the limiting hydrogen to the pellet: i.e., the dissolved hydrogen concentration remains closer to its equilibrium value over the entire pellet length. For the double-tube inlet, hydrogen supplied to the pellet from the liquid film that is consumed is not replenished rapidly enough. This results in a film hydrogen concentration that decreases down the pellet. A secondary effect is that the higher required flow rates for the single inlet increases the liquid-to-solid mass transport coefficient (Funk, 1990).

For the unsaturated liquid feed, the number of liquid films has little effect, as demonstrated in Figure 14. Compared to the presaturated liquid feed case, less hydrogen is supplied from the liquid flowing over the pellet. Thus, changes in the transport properties of the liquid film should have less impact. As a result, there is good agreement between the rates for the two inlets as the wetting efficiency is varied. From another perspective, if the liquid velocity is sufficiently high, the unsaturated liquid acts as a barrier to the transport of gas-phase hydrogen. Thus, for a volatile reactant-limited system, the most important property of this film is how much of the external catalyst surface it blocks. Thus, the total coverage, not the number of liquid rivulets, is the important factor.

Film flow dynamics and wetting

In the above analysis the single-pellet rate data was interpreted by considering the degree of wetting as an independent variable. The data, however, reveal a rather complex dependence of the degree of wetting on the truly independent hydrodynamic variable, the volumetric liquid flow rate.

The simplicity of the flow configuration used in the experiment permits an approximate analysis using the model for laminar flow of a liquid film down a wall. Estimation of the film Reynolds number (Re) helps determine the nature of the flow. For film flow down a wall Re is given by $4\Gamma/\mu$, where the mass flow rate per unit film width, Γ, is equal to $\rho q_r/W$, where ρ is the liquid density and W is the film width. For the conditions of our experiments we estimate $Re = 10$–100. For values of Re less than approximately 25, the liquid stream is laminar with no rippling. For Re values greater than approximately 1,000, the film is turbulent. Between these two regimes, the liquid film is laminar and rippled (Bird et al., 1960). Indeed, ripples in the film were visible to the naked eye at the higher flow rates. Our analyses also reveal that the film thickness is much less than its width and the pellet radius. This fact is exploited below.

In all of the experiments, the dependence of the degree of wetting on the volumetric liquid flow rate exhibits a consistent functional form. This form holds for the single (Figure 10) or double inlet data (Figure 4) and for runs in which the overall rate is high or low. Between zero flow rate and the lowest, nonzero flow rate data point, wetting increases dramatically. Beyond this narrow range of low liquid flow rates, the data exhibit an almost linear dependency of wetting efficiency on flow rate. Finally, at a sufficiently high flow rate the degree of wetting either approaches a constant value that is less than 0.5 for the single film cases or equal to unity for the two-film cases.

Comparison of the wetting-flow rate data for the single inlet (Figure 10) and double inlet (Figure 4) reveals very good agreement under the conditions of negligible reaction rate, i.e., the nitrogen gas-phase experiments. For example, 50% wetting is achieved with the single film at about 0.2 mL/s; complete wetting is achieved with two films at about 0.4 mL/s. Thus, the film flow is quite reproducible despite the rough, porous, curved surface. However, the good agreement between the single and double inlet wetting behavior does not hold if the rate is high (pure AMS and a hydrogen gas phase). This indicates an apparent impact of reaction on wetting. This point is considered in more detail below.

A large number of variables may have an impact on the rivulet width along the active section:

- The inlet configuration—inlet tube diameter and position relative to the pellet surface, the length of the prewetting section
- The pellet features—its surface roughness, porous structure, degree of pore filling by the liquid, cyclindrical shape and diameter
- The physical properties of the liquid—viscosity, density, surface tension, and apparent contact angle with the surface
- Operating conditions—liquid flow rate, temperature, and the surrounding gas composition.

Because of the complex nature of the porous liquid-filled surface of the pellet, the notion of a single contact angle or even its measurement is quite tenuous. Nevertheless, our visual inspection revealed that the liquid wetted the surface quite well and that an apparent contact angle (ignoring any complex features on the porous surface) was very small. Moreover, the rivulets formed were very thin, as estimated using the simple film model.

If we ignore the inlet configuration effects and assume that the surface of the porous, liquid-filled support behaves as a flat, nonporous solid, the rivulet can be modeled following the analyses of rivulet flow on an inclined surface by Towell and Rothfeld (1966) and Bentwich et al. (1976). An extension of their analysis gives the following dependence of the rivulet width (W) on the kinematic viscosity (ν), flow rate (q_r) and contact angle (θ):

$$W = \left[\frac{24\nu}{g}\right]^{1/4}\left[\frac{q_r}{F(\theta)}\right]^{1/4} \tag{9}$$

Thus, the rivulet width (W) is proportional to the one-fourth power of the volumetric flow rate and is a quite complex function of the contact angle. $F(\theta)$ is a function of the contact angle given by Towell and Rothfeld (1966). They show that $F(\theta)$ is a sensitive function of θ for small θ. The $W \propto q_r^{1/4}$ dependence closely resembles the functional dependence of the degree of wetting (i.e., $E_w = W/\pi d_p$) on flow rate in Figures 4 and 10. We fitted these data using Eq. 9 and found an excellent qualitative agreement. Moreover, $F(\theta)$ was determined to be on the order of 10^{-5} to obtain a good fit. It is easy to show that $F(\theta)$ approaches zero as θ approaches zero. This indicates that the apparent contact angle on the porous surface is indeed very small, confirming our observations discussed above.

In our previous studies (Zimmerman et al., 1987; Harold and Ng, 1987; Funk et al., 1989, 1990), wetting efficiency was estimated based on a model which assumes that the liquid on the catalyst surface can be viewed as a flat, thin film. Without repeating the theory here, it is sufficient to point out that this film model predicts a linear dependence of wetting efficiency on liquid flow rate. As expected, the model fails to predict the abrupt drop in the wetting for flow rates between zero and the lowest flow rate measured. A rivulet with a circular arc is clearly a better representation of the actual flow than a very narrow film at these low liquid flow rates. However, the E_w data for the ranges $0.02<q_r<0.4$ mL/s in Figure 4 and $0.02<q_r<0.2$ mL/s in Figure 10 exhibit an almost linear dependence of wetting efficiency on flow rate. This lends support for the use of the film flow model in estimating wetting efficiency at sufficiently high liquid flow rates.

Finally, we should point out that one should exercise caution in comparing the data for $q_r>0.2$ mL/s in Figure 10 with either the film model or rivulet model predictions. In this region, a one-dimensional film flow model clearly is not applicable. This might be due to the fact that, with the single-tube inlet, the flow is basically a two-dimensional flow. That is to say, there is an inlet effect. It is not clear whether the rivulet model is still applicable. It is applicable if the wetting efficiency increases with the liquid flow rate, since the rivulet model predicts that $E_w \propto q_r^{1/4}$. However, a wetting efficiency which plateaus out at about $E_w=0.5$ is probably a result of the two-dimensional nature of the flow. The data does not permit an unequivocal conclusion.

Impact of reaction on degree of wetting

To complicate matters further, the data reveal that the degree of wetting depends on the reaction rate. The degree of wetting was observed to be consistently higher when the gas phase consisted of pure nitrogen as compared to runs with pure hydrogen, with all other conditions fixed. This observation was true for both the single-inlet (Figure 10) and double-inlet (Figure 4) experiments. For example, a comparison of the wetting-flow rate data for the double- and single-tube inlets (Figures 4 and 10) using a hydrogen gas phase and pure AMS liquid phase reveals significant differences in the wetting behavior. Complete wetting was achieved with two films at a flow rate of approximately 0.45 mL/s (Figure 4). Under the same conditions, the single film only wetted about 35% of the surface at half that flow rate (Figure 10). Ideally, with the two films positioned at the opposite sides of the pellet, complete wetting should occur at a flow rate that is twice the flow rate needed to wet half the pellet with the single film. Such was the case with the nitrogen gas phase.

Several mechanisms may explain this wetting behavior. The first class of mechanisms are direct. The most logical is that a switch in the gas composition from nitrogen to hydrogen may change the surface tension or contact angle. However, the influence of the gas composition on surface tension is negligible (Weast, 1982; Reid et al., 1977). Another direct mechanism is an influence of the contact angle, given the sensitive dependence of the degree of wetting of a rivulet on the contact angle (Eq. 9; Towell and Rothfeld, 1966).

A second class of mechanisms indirectly impact the degree of rivulet wetting by way of the reaction heat effects. These are thermocapillarity, vapor thrust, or a change in the nature of the surface due to local vaporization. The former two processes have been shown to enhance the formation of a dry patch during film flow on a heated surface (Zuber and Straub, 1966; Chung and Bankoff, 1980).

The main premise for these complex nonisothermal processes is as follows. AMS hydrogenation is exothermic ($\Delta H=-108.8$ kJ/mol). A local temperature rise will occur without efficient removal of the heat generated. A temperature rise is most likely to occur near the nonwetted surface of the partially wetted pellet. In this locale, the supply rate of the limiting reactant hydrogen is highest but the external removal of energy is poorer than on the wetted surface. There are two consequences: 1. the establishment of a temperature gradient and 2. the vaporization of some liquid from the rivulet or from liquid in the pores exposed directly to the gas. It is not clear whether the magnitude of such a temperature rise is necessary to have an impact. Unfortunately, we did not measure the pellet temperature. In current work that addresses the very issue of vaporization in multiphase catalytic reactions involving volatile liquid feeds, we measure the pellet temperature and intrapellet liquid holdup (Watson and Harold, 1990).

The existence of a local temperature rise near the contact line of the rivulet could create a lateral surface force due to a surface tension which increases with temperature. This is the thermocapillary effect. As shown above, the one-dimensional flow of a rivulet down a vertical surface results in a cross-section of a circular arc. Moreover, the rivulet width is independent of surface tension due to the constant pressure in the lateral direction. However, a local temperature gradient which decreases from the nonwetted to the wetted surface will introduce a lateral force which serves to reduce the degree of wetting.

Vaporization of a fraction of liquid from the rivulet near the contact line creates a force acting of the rivulet. This is the vapor thrust effect. This too would serve to reduce the coverage of the rivulet and distort its circular arc cross-sectional shape.

Finally, vaporization of liquid at the exposed pose mouths may change the nature of the surface and thus the wetting behavior of the rivulet. Harold (1988) showed for an exothermic decomposition reaction that the heat of reaction can cause vaporization of intrapellet liquid. At steady state, the vaporization process is balanced by the supply of liquid into the pores by capillary-driven imbibition. Although AMS is rather nonvolatile at the conditions of the experiment (40°C), there is evidence that some vaporization occurred. First, a visual comparison between the nature of the nonwetted surface in experiments with the nitrogen gas phase (i.e., negligible rate) and hydrogen gas phase (high rate) revealed one key difference. The surface was darker in the case of the nitrogen experiments. This indicated that the liquid held in the pores was located very near the surface. The lighter "greyish" appearance of the surface in the hydrogen gas-phase experiments indicated that the liquid receded some distance into the pores under these conditions. Second, in recent transient experiments of AMS hydrogenation in our laboratory, significant vaporization and temperature rise was observed (Watson and Harold, 1990). For example, a pellet prefilled with AMS and then exposed to pure hydrogen exhibited a temperature rise of nearly 100°C and dried out in minutes.

Conclusions

The impact of partial external wetting on catalyst performance has been investigated using a novel single-pellet experiment. The reactor used in this study simulates the local environment within a packed-bed, trickling-flow reactor but has a more well defined flow system. This permitted for the first time the direct measurement of the fractional liquid coverage under reaction conditions, and thus enabled a more thorough analysis of the reaction-transport-wetting interactions.

There are some noteworthy conclusions. If both the volatile and nonvolatile reactants are more effectively supplied through the wetted portion of catalyst surface, the overall reaction rate increases monotonically with liquid flow rate (or liquid coverage). However, if the more effective supply route for the volatile reactant is through the nonwetted surface, a maximum in the reaction rate occurs at an intermediate level of wetting. This maximum results from a competition between two different limiting regimes. At sufficiently low liquid coverages, the catalyst is limited by the supply of the nonvolatile reactant, whereas at higher coverages the pellet is volatile-reactant-limited. The data provide concrete evidence for the effectiveness enhancement phenomenon predicted previously by models of the partially wetted catalyst pellet (e.g., Harold and Ng, 1987; Funk et al., 1988, 1989).

An intriguing coupling between the rate of reaction and the degree of wetting was also observed. For the same total liquid flow rate, wetting was consistently lower under conditions that gave a high reaction rate. We believe that this is caused by an indirect, nonisothermal process related to the exothermic nature of the reaction used in this study. However, due to the complexity of the rivulet dynamics and its coupling to the reaction, we could not pinpoint the exact cause. Because of the industrial significance of nonisothermal phenomena such as hot spot formation, these problems clearly warrant further study.

Many of the experimental observations made in this study could not have been obtained with a packed-bed reactor or other more traditional techniques. Although the hydrogenation of α-methylstyrene on Pd/Al_2O_3 is not of commercial interest, it has several features that are typical of many industrial multiphase reactions. Moreover, although rivulet flow is just one flow type in the trickle-bed reactor, its relative simplicity afforded a detailed examination of the impact of external wetting on catalyst performance. Given these facts and the rather broad range of qualitatively different behaviors observed, we feel that the single-pellet reactor approach to studying multiphase reactions has promising utility in addressing other issues, such as intrapellet vaporization and the effect of wetting on selectivity. Efforts are currently under way to use the single-pellet reactor approach to investigate such problems (e.g., Watson and Harold, 1990).

Acknowledgment

This research was supported by National Science Foundation Grant No. CBT-8700554. We are grateful to Mobil Oil (Engineering, Princeton, NJ) for carrying out the electron microprobe scans of the catalyst pellets.

Notation

C = concentration
C_A = concentration of AMS
C_{bA} = bulk concentration of AMS
C_H = concentration of hydrogen
C_{bH} = bulk concentration of hydrogen
d_p = pellet diameter
D_{eH} = effective diffusivity of hydrogen
E_w = wetting efficiency
g = acceleration due to gravity
k' = pseudo first-order rate constant
k_{gls} = overall mass transport coefficient
k_r = surface reaction rate constant
K_A = adsorption equilibrium constant for AMS
m_{cat} = mass of catalyst
q_r = liquid flow rate
r_{int} = intrinsic reaction rate
r_{obs} = observed reaction rate
R_p = radius of pellet
Re = Reynolds number
S_x = external surface area of pellet
Sh' = modified Sherwood number
t = time
V_{liq} = average liquid system volume
V_p = pellet volume
W = film width

Greek letters

Γ = mass flow rate per unit film width
δ = maximum film thickness
δ = average film thickness
ϵ = porosity of pellet
η = effectiveness factor
μ = viscosity
ν = kinematic viscosity
θ = contact angle
ρ = liquid density
ρ_p = pellet density
ϕ = Thiele modulus
Φ = Weisz-Prater modulus

Literature Cited

Babcock, B. D., G. T. Mejdell, and O. A. Hougen, "Catalyzed Gas-Liquid Reactions in Trickling-Bed Reactors," *AIChE J.*, **3**, 366 (1957).

Bentwich, M., D. Glasser, J. Kern, and D. Williams, "Analysis of Rectilinear Rivulet Flow," *AIChE J.*, **22**, 772 (1976).

Bird, R. B., W. E. Stewart, and E. N. Lightfoot, *Transport Phenomena*, Wiley, New York (1960).

Capra, V., S. Sicardi, A. Gianetto, and J. M. Smith, "Effect of Liquid Wetting on Catalyst Effectiveness in Trickle-Bed Reactors," *Can. J. Chem. Eng.*, **60**, 282 (1982).

Chung, J. C., and S. G. Bankoff, "Initial Breakdown of a Heated Liquid Film in Cocurrent Two-Component Annular Flow: II. Rivulet and Drypatch Models,"*Chem. Eng. Comm.*, **4**, 455, (1980).

Cini, P., S. Blaha, M. P. Harold, and K. Venketaraman, "Preparation and Characterization of the Catalytic Ceramic Tube for Use as a Multiphase Catalyst," No. 133e, AIChE Annual Meeting, San Francisco (1989).

Dudukovic, M. P., "Catalyst Effectiveness Factor and Contacting Efficiency in Trickle-Bed Reactors," *AIChE J.*, **23**, 940 (1977).

Froment, G. F., and K. B. Bischoff, *Chemical Reactor Analysis and Design*, Wiley, New York (1979).

Funk, G. A., "Effect of Wetting on Catalytic Gas-Liquid Reactions," PhD Diss., Univ. of Massachusetts, Amherst (1990).

Funk, G. A., M. P. Harold, and K. M. Ng, "Effectiveness of a Partially Wetted Catalyst for Bimolecular Reaction Kinetics," *AIChE J.*, **34**, 1361 (1988).

Funk, G. A., M. P. Harold, and K. M. Ng, "Reactant Adsorption Effects on Partially Wetted Catalyst Performance," *Chem. Eng. Sci.*, **44**, 2509 (1989).

Funk, G. A., M. P. Harold, and K. M. Ng, "A Novel Model for Reaction in Trickle Beds with Flow Maldistribution," *Ind. Eng. Chem. Res.*, **29**, 738 (1990).

Gabbito, J. F., M. A. Laborde, and N. O. Lemcoff, "Effectiveness

Factor and Selectivity For Partially Wetted Catalyst Pellets in a Parallel Reaction System," *Lat. Am. J. Heat and Mass Trans.*, **9**, 75 (1986).
Germain, A. H., A. G. Lefebvre, and G. A. L'Homme, "Experimental Study of a Catalytic Trickle Bed Reactor," *Amer. Chem. Soc. Symp. Ser.*, **133**, 164 (1974).
Gianetto, A., G. Baldi, V. Specchia, and S. Sicardi, "Hydrodynamics and Solid-Liquid Contacting Effectiveness in Trickle-Bed Reactors," *AIChE J.*, **24**, 1087 (1978).
Goto, S., A. Lakota, and J. Levec, "Effectiveness Factors of nth Order Kinetics in Trickle-Bed Reactors," *Chem. Eng. Sci.*, **36**, 157 (1981).
Harold, M. P., "Partially Wetted Catalyst Performance in the Consecutive-Parallel Network," *AIChE J.*, **34**, 980 (1988).
Harold, M. P., and K. M. Ng, "Effectiveness Enhancement and Reactant Depletion in a Partially Wetted Catalyst," *AIChE J.*, **33**, 1448 (1987).
Harold, M. P., P. Cini, B. Patenaude, and K. Venkataraman, "The Catalytically Impregnated Ceramic Tube: An Alternative Multiphase Reactor," *AIChE Symp. Ser.*, R. Govind, ed., **85**, 26 (1989).
Herskowitz, M., "Wetting Efficiency in Trickle-Bed Reactors. The Overall Effectiveness Factor of Partially Wetted Catalyst Particles," *Chem. Eng. Sci.*, **36**, 1665 (1981).
Herskowitz, M., and S. Mosseri, "Global Rates of Reaction in Trickle-Bed Reactors: Effect of Gas and Liquid Flow Rates," *Ind. Eng. Chem. Fundam.*, **22**, 4 (1983).
Herskowitz, M., and J. M. Smith, "Trickle-Bed Reactors: A Review," *AIChE J.*, **29**, 1 (1983).
Herskowitz, M., R. G. Carbonell, and J. M. Smith, "Effectiveness Factors and Mass Transfer in Trickle-Bed Reactors," *AIChE J.*, **25**, 272 (1979).
Leung, P. C., F. Recasens, and J. M. Smith, "Hydration of Isobutene in a Trickle-Bed Reactor," *AIChE J.*, **33**, 996 (1987).
Mata, A. R., and J. M. Smith, "Oxidation of Sulfur Dioxide in a Trickle-Bed Reactor," *Chem. Eng. J.*, **22**, 229 (1981).
Mears, D. E., "The Role of Liquid Holdup and Effective Wetting in the Performance of Trickle-Bed Reactors," *Amer. Chem. Soc. Symp. Ser.*, **133**, 218 (1974).
Mills, P. L., and M. P. Dudukovic, "A Comparison of Current Models for Isothermal Trickle-Bed Reactors," *Amer. Chem. Soc. Symp. Ser.*, **237**, 37 (1984).
Morita, S., and J. M. Smith, "Mass Transfer and Contacting Efficiency in a Trickle-Bed Reactor," *Ind. Eng. Chem. Fundam.*, **17**, 113 (1978).
Ng, K. M., and C. F. Chu, "Trickle-Bed Reactors," *Chem. Eng. Prog.*, **38**, 55 (1987).
Ring, Z. E., and R. W. Missen, "Trickle-Bed Reactors: An Experimental Study of Partial Wetting Effect," *AIChE J.*, **35**, 1821 (1989).
Ramachandran, P. A., and J. M. Smith, "Effectiveness Factors in Trickle-Bed Reactors," *AIChE J.*, **25**, 538 (1979).
Reid, R. C., J. M. Prausnitz, T. K. Sherwood, *The Properties of Gases and Liquids*, McGraw-Hill, New York (1977).
Ruecker, C. M., and A. Akgerman, "Determination of Wetting Efficiencies for a Trickle-Bed Reactor at High Temperatures and Pressures," *Ind. Eng. Chem. Res.*, **26**, 164 (1987).
Sakornwimon, W., and N. D. Sylvester, "Effectiveness Factors for Partially Wetted Catalysts in Trickle-Bed Reactors," *Ind. Eng. Chem. Proc. Des. Dev.*, **21**, 16 (1982).
Satterfield, C. N., A. A. Pelossof, and T. K. Sherwood, "Mass Transfer Limitations in a Trickle-Bed Reactor," *AIChE J.*, **15**, 226 (1969).
Satterfield, C. N., "Trickle-Bed Reactors," *AIChE J.*, **21**, 209 (1975).
Satterfield, C. N., and F. Ozel, "Direct Solid-Catalyzed Reaction of a Vapor in an Apparently Completely Wetted Trickle-Bed Reactor," *AIChE J.*, **19**, 1259 (1973).
Sedricks, W., and C. N. Kenney, "Partial Wetting in Trickle-Bed Reactors—The Reduction of Crotonaldehyde Over a Palladium Catalyst," *Chem. Eng. Sci.*, **28**, 559 (1973).
Shoemaker, D. P., C. W. Garland, J. I. Steinfeld, and J. W. Nibler, *Experiments in Physical Chemistry*, McGraw-Hill, New York (1981).
Towell, G. D., and L. B. Rothfeld, "Hydrodynamics of Rivulet Flow," *AIChE J.*, **12**, 972 (1966).
Tukac, V., I. Mazzarino, G. Baldi, A. Gianetto, S. Sicardi, and V. Specchia, "Conversion Rates in a Laboratory Trickle-Bed Reactor During the Oxidation of Ethanol," *Chem. Eng. Sci.*, **41**, 17 (1986).
Turek, F., and R. Lange, "Mass Transfer in Trickle-Bed Reactors at Low Reynolds Number," *Chem. Eng. Sci.*, **36**, 569 (1981).
Van Landegham, H., "Multiphase Reactors: Mass Transfer and Modeling," *Chem. Eng. Sci.*, **35**, 1912 (1980).
Watson, P., and M. P. Harold, "Exothermic Multiphase Reaction with Vaporization in the Single Catalytic Pellet: Modelling and Experiment," No. 126d, Annual AIChE Meeting, Chicago (1990).
Weast, R. C., ed., *Handbook of Chemistry and Physics*, **63**, CRC Press, Boca Raton (1982).
Weisz, P. B., and C. D. Prater, "Interpretation of Measurements in Experimental Catalysis," *Adv. Catal.*, **6**, 143 (1954).
Yentekakis, I. V., and C. G. Vayenas, "Effectiveness Factors for Reactions Between Volatile and Nonvolatile Components in Partially Wetted Catalysts," *Chem. Eng. Sci.*, **42**, 1323 (1987).
Zuber, N., and F. W. Straub, "Stability of Dry Patches Forming in Liquid Films Flowing Over Heated Surfaces," *Int. J. Heat Mass Trans.*, **9**, 897 (1966).
Zimmerman, S. F., C. F. Chu, and K. M. Ng, "Axial and Radial Dispersion in Trickle-Bed Reactors with Trickling Gas-Liquid Down-Flow," *Chem. Eng. Comm.*, **50**, 213 (1987).

Manuscript received July 6, 1990, and revision received Dec. 11, 1990.